

Synthesis of Highly Conductive Stretchable Interconnect with Polymer Composite  
and its Evaluation Against Market-Available Materials

by

Mayukh Nandy

A Thesis Presented in Partial Fulfillment  
of the Requirements for the Degree  
Master of Science

Approved July 2020 by the  
Graduate Supervisory Committee:

Hongbin Yu, Chair  
Candace Chan  
Hanqing Jiang

ARIZONA STATE UNIVERSITY

August 2020

## ABSTRACT

Flexible conducting materials have been in the forefront of a rapidly transforming electronics industry, focusing on wearable devices for a variety of applications in recent times. Over the past few decades, bulky, rigid devices have been replaced with a surging demand for thin, flexible, light weight, ultra-portable yet high performance electronics. The interconnects available in the market today only satisfy a few of the desirable characteristics, making it necessary to compromise one feature over another. In this thesis, a method to prepare a thin, flexible, and stretchable inter-connect is presented with improved conductivity compared to previous achievements. It satisfies most mechanical and electrical conditions desired in the wearable electronics industry. The conducting composite, prepared with the widely available, low cost silicon-based organic polymer - polydimethylsiloxane (PDMS) and silver (Ag), is sandwiched between two cured PDMS layers. These protective layers improve the mechanical stability of the inter-connect. The structure can be stretched up to 120% of its original length which can further be enhanced to over 250% by cutting it into a serpentine shape without compromising its electrical stability. The inter-connect, around 500  $\mu\text{m}$  thick, can be integrated into thin electronic packaging. The synthesis process of the composite material, along with its electrical and mechanical and properties are presented in detail. Testing methods and results for mechanical and electrical stability are also illustrated over extensive flexing and stretching cycles. The materials put into test, along with conductive silver (Ag) - polydimethylsiloxane (PDMS) composite in a sandwich structure, are copper foils, copper coated polyimide (PI) and aluminum (Al) coated polyethylene terephthalate (PET).

## ACKNOWLEDGMENTS

I would like to express my heartfelt gratitude to Dr. Hongbin Yu for his unwavering support throughout this endeavor. Without his guidance and exemplary knowledge, this thesis would not have been possible.

I would like to thank Dr. Candace Chan for the use of her lab space and Bending Fatigue Testing Machine for mechanical durability testing at the School for Engineering of Matter, Transport and Energy at Arizona State university.

I wish to acknowledge Dr. Lenore Dai for the use of the Ta.XT plus Texture Analyzer in the strain measurement experiment and Arizona State University's Center for Solid State Research for the use of the facility for material characterization.

I would like to thank Dr. Hanqing Jiang for making time to serve on my committee and broadening my knowledge with his questions and comments.

I acknowledge the use of four-point probe station within the ASU NanoFab supported in part by NSF program NNCI-ECCS-1542160.

I would like to thank my colleagues in Dr. Hongbin Yu's group: Todd Houghton and Yanze Wu.

This work was sponsored by the U.S. Government under contract 2019-19071100001 -- Task order 001.

## TABLE OF CONTENTS

	Page
LIST OF TABLES.....	v
LIST OF FIGURES.....	vi
CHAPTER	
1 INTRODUCTION .....	1
2 BACKGROUND LITERATURE .....	3
Percolation Theory .....	3
Previous Work on Conducting Composite .....	4
State of the Art.....	7
3 METHODOLOGY .....	9
Preparation of Ag-PDMS Composite .....	9
Preparation of Base PDMS Film.....	10
Preparation of Sandwich Structure .....	11
Serpentine Structure .....	12
4 TESTS .....	13
Bending Fatigue Test .....	13
Stretching Test.....	14
5 RESULTS AND DISCUSSION.....	15
Ag-PDMS Composite .....	15
Cu Foil, Single-sided Cu Coated PI, Al Coated PET .....	20
Serpentine Structure .....	22
6 CONCLUSION .....	24

CHAPTER	Page
7 FUTURE SCOPE OF WORK.....	25
REFERENCES .....	26

## LIST OF TABLES

Table		Page
1.	State Of The Art Achievements in Stretchable Interconnects in Recent Years.....	7
2.	Electrical Characterization of Various Materials Used as Interconnects .....	20
3.	Serpentine Structures Of Materials and Their Measured Resistance.....	23

## LIST OF FIGURES

Figure	Page
1. Percolation Curve for Conducting Filler in Polymer Composite.....	3
2. Conductivity Flow Chart for Carbon and Metal-based Conducting Fillers.....	8
3. Different Layers in the Sandwich Structure .....	9
4. Preparation of Highly Conductive Ag-PDMS Composite Paste.....	10
5. Preparation of Sandwich Structure.....	10
6. Top and Bottom Layer View of the Sandwich Structure.....	11
7. Serpentine Shape Cut Out of an Ag-PDMS Sandwich Structure .....	12
8. Top and Cross-Sectional Optical Microscopic View of Sandwich Structure.....	16
9. Bending Fatigue Test Setup for 90° Bend .....	17
10. Stretching Test Setup .....	18
11. Naked Eye and Optical Microscopic View of the Ruptured Edge .....	19
12. Plot of $\Delta R/R_0$ against Strain% .....	19
13. SEM Image of Cracks from Extensive Bending.....	21
14. Bending Fatigue Test Setup for 45° Bend .....	22
15. Serpentine Structure Cut Out of a Cu Foil.....	23

## CHAPTER 1

### INTRODUCTION

Over the past decades, foldable electronics have become a major area of research in the electronics industry. Our devices are getting smaller, more portable and the need for flexible electronics is booming for various applications. While a major part of the research is being performed on high performance flexible and foldable printed circuit boards (PCB) and batteries, the materials used as the interconnects has remained largely under-explored. The thin metal sheets available in the market today are an ideal choice for such applications owing to their high conductivity. The lifetime and mechanical stability of these materials are most important before considering them for integration into flexible electronic packages. Materials like thin copper foils provide metallic conductivity but cannot be stretched or bent repeatedly over the lifetime of the product owing to bending fatigue and ultimately mechanical deformation leading to electrical failure. On the other hand, stretchable metal polymer composite structures previously explored by researchers in this industry failed to achieve foil-like thickness or high conductivity to compete with metal counterparts [1][2][3][4]. Stretchable interconnects are mainly characterized by their ability to bend, fold, compress or stretch while maintaining their electrical stability and mechanical durability even under considerable deformations. Hence, a trade-off between the mechanical and electrical properties has always put the researchers in a dilemma while choosing interconnects for potential applications in flexible and stretchable electronics. In this research, we aim to fabricate a highly conductive interconnect, using polydimethylsiloxane (PDMS) and silver (Ag), that is both extensively flexible and stretchable. The conducting composite



paste using Ag and PDMS is sandwiched between two cured PDMS layers to provide durability to the interconnect. The prepared sample is subject to extensive bending fatigue tests to note any deformations. Stretchability tests are also conducted to find out the elongation at break and the change in resistance with elongation. Commercially available flexible interconnect materials like copper (Cu) foil, copper (Cu) coated polyimide (PI) and aluminum (Al) coated polyethylene terephthalate (PET) are also tested under the same standards for flexibility and elasticity. The samples under test are then examined under an optical and a scanning electron microscope (SEM) for bends, creases, cracks, and other mechanical deformations that occurred in the process.

## CHAPTER 2

### BACKGROUND LITERATURE

#### 2.1 Percolation Theory

The electrical behavior of conducting polymer composites can be explained with percolation theory. Conducting polymer composites comprise of conducting filler material amidst insulating polymer matrices where the conductive filler can alter the electrical properties of the host polymer matrix. Below a critical percentage of conducting filler content, also known as percolation threshold, electron paths are not formed, and the insulating properties of the polymer matrix dominate. After gradually increasing the conducting filler beyond the threshold, a percolation transition occurs with a huge increase in electrical conductivity of the polymer composite by several orders of magnitude. Once this transition occurs, the fillers form a continuous network to provide a percolation path for the electrons to conduct. The percolation threshold varies with filler materials. After a path is formed, increasing filler content in the composite increases the electrical conductivity until it reaches a percolation limit. Beyond this limit, no significant change in conductivity is observed with further increasing filler content. This classical percolation theory only applies to homogeneous infinite networks [5][6].

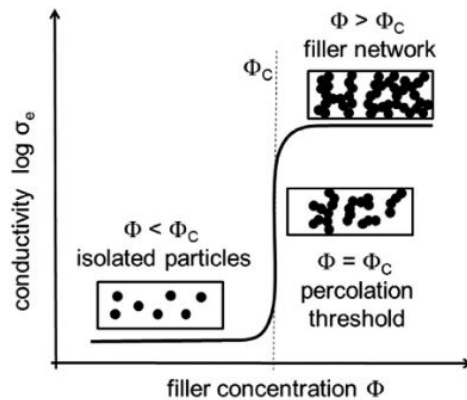


Fig. 1. Schematic percolation curve for conducting filler in polymer composite [5].

## 2.2 Previous Work on Conducting composite

In the recent years, various conducting materials such as flakes, nanowires(NWs) and nanocrystals(NCs), graphene sheets and Carbon Nano Tube(CNT) based polymer composites alongside thin metal sheets have been used for a spectrum of stretchable and flexible applications, such as strain sensors for healthcare and sports, artificial arms, radiofrequency antennas, foldable displays and soft robotics [7][8][9][10][11][12][13][14]. These filler conducting materials are mixed into polymer matrices to prepare elastic yet conductive composites. Materials chemistry has an important role to play in developing new conducting fillers or soft elastic polymers or even integrating different combinations of filler and polymer [15] to further improvise on the stretchable interconnects that we have today. The other important consideration while advancing in this field is taking either “materials that can stretch” or “structures that can stretch” approach [16]. While both strategies aim at the same category of applications, each approach comes with minor to significant benefits and drawbacks over the other.

Nanocrystals and nanowires have shown a lot of potential in conductive stretchable materials over the years. Their high conductivity and ability to maintain the conducting path upon stretching have made them a preferred choice for many applications. Some processes involving silver nanocrystals require intense localised heating, induced by intense pulsed light (IPL) irradiation, to achieve effective sintering for improved conduction [1]. Silver nanowires embedded in the surface layer of polydimethylsiloxane (PDMS) have also been attempted successfully with low sheet resistance and electrical stability over several stretching cycles [17]. Efforts have also been made to further improve thermal and electrical stability of silver nanowire network

by integrating graphene oxide intermediate layers [18]. However, the complexity in the process of sintering NCs and cost of synthesis and low yield of NWs [19] makes it significantly challenging to make these time-consuming processes commercially and practically viable. A simpler method was developed by Yougen Hu, et al. to prepare a sandwich structure with Ag-PDMS, primarily for strain sensor applications [20].

Silver has been replaced with copper nanowires for comparable metallic conductivity. But, the tendency of copper to oxidise quickly was well as the treatment process of CuNWs/PDMS films with IPL irradiation, to achieve an enhanced conductive layer, makes them practically implausible [21]. Low cost method to prepare silver flakes mixed into a polyvinyl alcohol (PVA) polymer matrix plasticized with phosphoric acid achieved high stretchability but exhibited moderate conductivity which increased with stretching, owing to improved orientation of the conducting filler particles in the sample when stretched [22]. Thermoplastic polyurethane (TPU) [23], Polyethylene terephthalate (PET) [24], other polymer matrices and tough hydrogels [25] have also been used as substrates for interconnects.

Carbon Nanotubes (CNTs) have been a popular choice for fabricating stretchable interconnects due to their mechanical robustness, high thermal and chemical stability, and elastic modulus. Y Zhang et al. [26] integrated aligned multi-walled carbon nanotubes (MWCNTs) into PDMS substrate. Although electrical stability was observed upon extensive stretching, their inferior conductivity in its original state remained an unresolved issue.

Additionally, there is a geometric engineering-based approach that many researchers take while developing interconnects for stretchable applications. Bi-axial in-

plane serpentine design with printed conducting ink integrated on the surface of a polymer matrix has been explored by John A. Rogers et al. [27]. Binary network structured polyurethane sponge–Ag nanowire– polydimethylsiloxane (PUS-AgNW-PDMS) stretchable conductors prepared through a solution-dipping method by Shu-Hong Yu and his team [28] helped achieve a electrically stable yet stretchable structure in 3-D but with unremarkable conductivity. Conducting composite pastes for printed stretchable conductors have also been developed to be printed into foldable designs, even in vertically stackable 3-D printing process, on stretchable substrates [29]. But their robustness over extensive bending and stretching over the lifetime of the interconnect is still unknown. Post-printing sintering required to remove the insulating impurity materials from the ink is an added time-consuming process [30]. Zig zag stripes of Polymer Gel/Metal Nanoparticle Composites in 3D [31], mesh structures, microcracks on thin Au films, longitudinal waves [32] are a few of structural designs attempted at making traditional conductors stretchable. Conductive elastomeric composite on a micro-pyramid array [33] and knitted fabrics made from highly conductive stretchable fibers synthesised by wet spinning has failed to maintain electrical stability with stretching [34]. To solve this problem, kirigami approach to pattern highly conductive stretchable interconnects for various applications in e-skin devices has become a popular area of research [35].

### 2.3 State of the Art

<b>Filler Material</b>	<b>Maximum Reported Conductivity S cm<sup>-1</sup></b>	<b>Substrate</b>	<b>Structure</b>	<b>Maximum Reported Stretchability (%)</b>	<b>Ref.</b>
Ag NPs	17460	PVDF-HFP	Knitted Fibers	50	[34]
Ag Nanoflakes+ NCS	2861.2	PDMS	Screen Printed on Rectangular PDMS Strip	50	[1]
Ag NPs	21000	PDMS	Ordered Zigzag Stripes in 3D	55	[31]
Ag NWs	46700	PUA	Ag NW Ink Screen Printed on PUA	80	[36]
Cu NWs	50000	PDMS	Rectangular Strips	70	[21]
GO/CNC	1105	Composite	Rectangular Strips	5	[2]
CNT	3.6	SEBS	Fibers	1320	[3]
CNT	2200	PDMS	Thin Films	150	[4]

Table 1. State of the art achievements in stretchable interconnects in recent years [36]. Abbreviations: Ag-Silver, NPs-NanoParticles, NCS-NanoCrystals, NWs-Nanowires, Cu-Copper, GO-GrapheneOxide, CNC-CelluloseNanoCrystals, CNT-CarbonNanoTubes, PVDF-HFP- Poly(vinylidene fluoride-co-hexafluoropropylene), PDMS- Polydimethylsiloxane, PUA- poly(urethane acrylate), SEBS- Styrene-ethylene-butylene-styrene.

Fig. 3 further categorises the results from Table 1, where carbon-based fillers for conductive composites achieve only up to few  $10^2$  S cm<sup>-1</sup> conductivity while metal-based

nanoparticles, nano or micro flakes, nanowires can reach much higher and even metal-like conductivity. The electrical conductivity is mainly determined by the intrinsic electrical behaviour of the embedded conducting filler in the percolation network along with their particle size and shape. One of the attempts taken previously by T. Houghton, et al. [21] to prepare a silver-polymer composite material to be used in capacitive wearable sensors achieved mechanical robustness and low-cost manufacturing. The composite was prepared by mixing silver flakes and poly(3,4-ethylenedioxythiophene) into a polyvinyl alcohol (PVA) polymer matrix plasticized with phosphoric acid. The resultant polymer showed a conductivity of  $85 \times 10^{-4} \text{ S cm}^{-1}$ . With 100% strain, resistivity showed a noticeable decrease by 29% owing to the increased bulk resistance and length. Over 400 stretching cycles, resistivity showed a small increase of  $6 \text{ } \Omega\text{cm}$ .

This research was performed to achieve metal-like conductivity in composite polymers along with physical robustness and electrical stability. Various sizes of Ag fillers were attempted in different concentration combinations with host polymer materials before achieving the aimed results with the Ag-PDMS conducting composite in a PDMS sandwich structure.

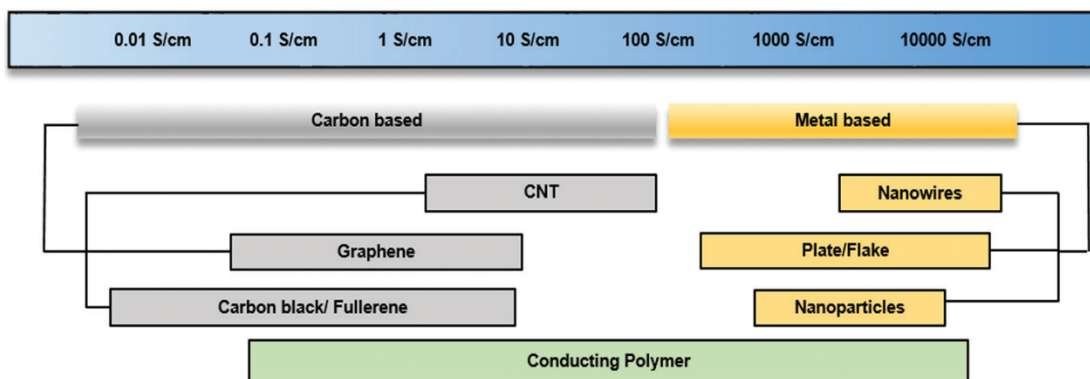


Fig. 2. Conductivity flow chart for carbon and metal-based conducting fillers in polymer composites [37]

## CHAPTER 3

### METHODOLOGY

A multi-layered yet thin, highly conductive, flexible, and stretchable material is prepared which can be used as interconnects. As illustrated in Fig.3, the structure consists of 3 layers with Ag-PDMS composite sandwiched between two layers of cured PDMS. The Ag-PDMS composite acts as the conducting layer while the cured PDMS is used for its mechanical robustness with extensive flexing, stretching and high temperature tolerance. The sandwich structure is necessary to protect the Ag-PDMS composite layer which is not cured due to the absence of a hardening agent.

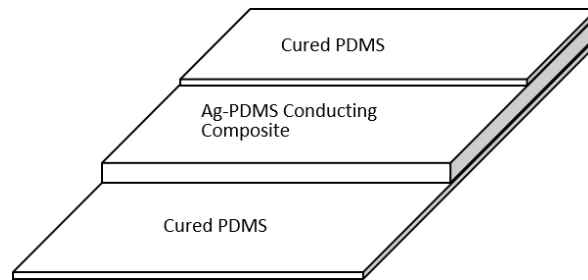


Fig. 3. Schematic Illustration of different layers in the sandwich structure

#### 3.1 Preparation of Ag-PDMS Composite

Silver flakes (Ag,  $<10\mu\text{m}$ , 99.9% metals basis) were procured from Sigma Aldrich and Polydimethylsiloxane (PDMS-Slygard 184) from Fisher Scientific. Silver flakes were mixed into PDMS in the ratio of 88% by weight. Methyl-Isobutyl-Ketone (MIBK) was added to the mixture as a solvent and sonicated for 70 mins. The procedure has been illustrated in Fig. 4. Silver flakes were used as the highly conductive filler. PDMS was used as the polymer matrix for its adhesive properties to bind the silver flakes together inside the sandwich structure.



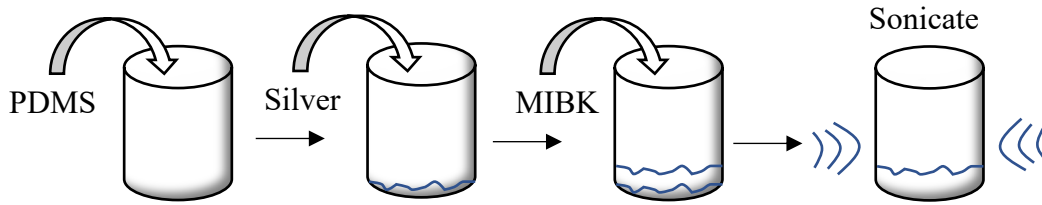


Fig. 4. Schematic illustration of preparing highly conductive Ag-PDMS composite paste

### 3.2 Preparation of Base PDMS Film

Polydimethylsiloxane (PDMS) was mixed with the curing agent in a ratio of 10:1 and spin coated inside a glass petri-dish. It was left to semi-dry in the heating oven at 60° C for 40 mins. 0.5cm x 2cm of 0.02mm thin copper foils were placed with 1cm on top of the semi-dry base PDMS film to connect with the Ag-PDMS composite and the rest of the length outside the petri-dish as tabs. The film is then left at 60° C for 60 mins to cure completely. Fig 5(a), (b), (c) and (d) illustrates the steps of preparation.

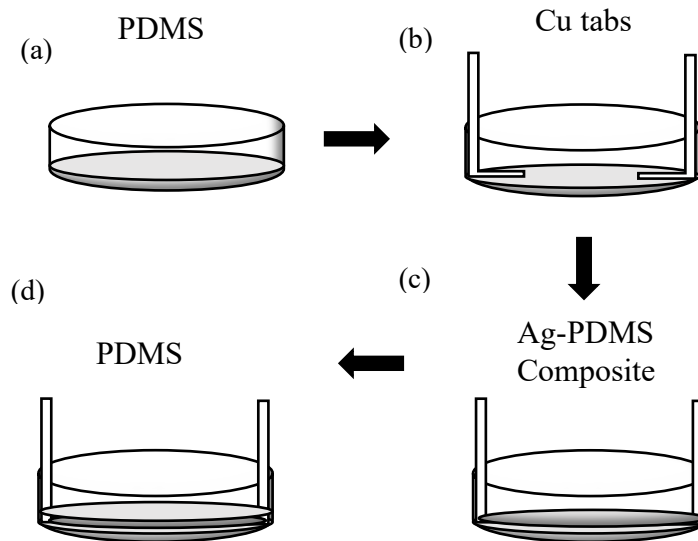


Fig. 5 Schematic Illustration for preparing the sandwich structure (a) PDMS and curing agent spin-coated on petri dish (b) Cu tabs placed on top of semi-dried PDMS such that only the bottom surface of Cu is attached to PDMS and fully cured. The top surface of the tab is kept exposed for contact with the conducting composite layer (c) Ag-PDMS composite in MIBK solvent spin-coated on top. (d) PDMS spin-coated as the final layer and cured.

### 3.3 Preparation of Sandwich Structure

The sonicated Ag-PDMS composite is spin coated on the cured PDMS substrate with Cu tabs attached on top and left to dry at room temperature for 48 hours. Another layer of PDMS with curing agent (10:1) is spin coated on top of it and left to dry at room temperature for 72 hours. The resultant cured sandwich structure is carefully peeled out of the petri-dish for measurements and tests. Fig. 6(a), (b) shows the top and bottom layer view of the sample.

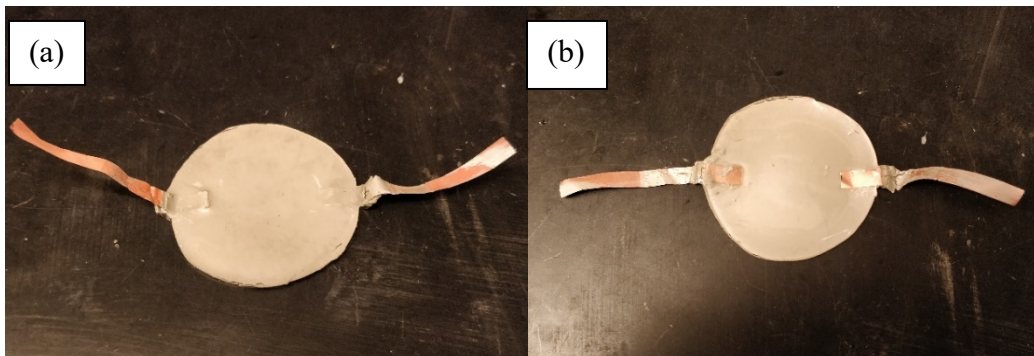


Fig. 6 (a) Top layer view of Ag-PDMS sandwich structure peeled out of petri-dish (b) Bottom layer view with copper foil tabs attached to PDMS

The thickness of the structure can be controlled by the spin coated top and bottom layers of PDMS without affecting the conducting composite layer in between. The bottom layer thickness is critical in a way that the composite spin coated on top of it contains MIBK which is a polymer solvent. Below a certain thickness of the base layer, it was observed that the MIBK tends to dissolve the cured PDMS, thereby spoiling the structure. On the other hand, the top layer can be made thinner with higher rpm in the spin coater as it coats a completely dried Ag-PDMS composite with the volatile MIBK evaporated during the drying process. This method of preparing the sandwich structure with consistent thickness and electrical and mechanical characteristics was repeated for several samples for tests.

### 3.4 Serpentine Structure

The sandwich structure is cut with scissors into a serpentine shape with 0.4cm width along the straight lines and 0.5cm around the curved edges as shown in Fig.7(a). The curves being the areas with maximum induced stress on stretching a serpentine structure, the greater width distributes the stress on a larger area leading to better mechanical stability.

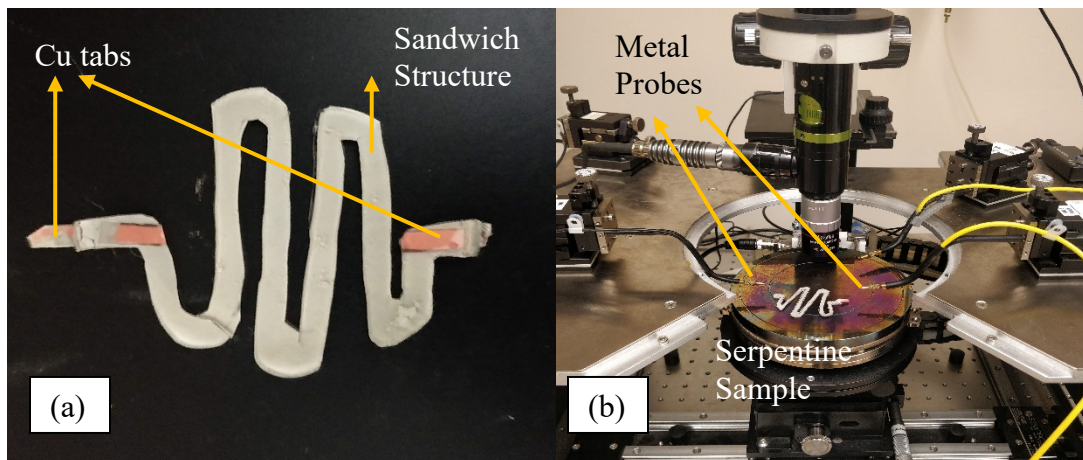


Fig. 7. (a) Serpentine shape cut out of an Ag-PDMS sandwich structure. (b) End to end resistance of the serpentine structure measured with a two-point DC probe.

## CHAPTER 4

### TESTS

5cm x 4cm samples were taken each of double-sided aluminum coated polyethylene terephthalate(PET) procured from Soteria Battery Innovation Group (Metallized Current Collector, 10 $\mu$ m PET, 500nm Al coating per side), single-sided copper coated polyimide(PI) procured from Dupont (Pyr lux AC, 18 $\mu$ m Cu, 25 $\mu$ m PI), 20 $\mu$ m thick Cu foil and a 4cm x 1.8cm sample of Ag-PDMS composite sandwich structure.

Another set of samples were cut into discs of radii 2.5 cm to be further made into serpentine structures. The disc shape was chosen for maximum utilization of the Ag-Composite sandwich structure prepared in a petri-dish of the same diameter. Hence, this was set as the standard shape for all materials under test.

#### 4.1 Bending Fatigue Test

The bending fatigue test is important to understand the ability of flexible materials to withstand extensive bending and flexing cycles over the course of a lifetime of the device. This test is particularly relevant in the flexible electronics industry today to test interconnects, batteries, and other components of wearable devices.

The samples were sandwiched between two polycarbonate sheets and their ends were clamped in between beams on the bending machine. The bending machine was operated for 10,000 cycles each at 45° with the distance between the two fixed ends 4.5 cm and 1.5 cm, respectively. This procedure was repeated with the same conditions at 90° bending angle. These different combinations of distance between the fixed clamps and bending angles were chosen to simulate the different conditions of light to extreme

bending that foldable interconnects might encounter in various applications. The SEM of the samples were taken before and after the tests precisely near the areas of maximum induced stress while bending to observe mechanical deformations.

#### 4.2 Stretching Test

The orientation of conducting filler in polymer-metal composites changes with applied tension and compression. This results in varying conductivity of the material under stress. Tensile testing of the samples was performed using a Ta.XT texture analyzer to analyze the change in resistance with elongation. The fabricated sample was elongated until its point of rupture. The material samples were attached to the analyzer using a pair of clamps which were covered with insulating tape to ensure electrical isolation from any metal component. Alligator clips from ohmmeter probes were attached to the metal tabs sticking out of the insulated clamps. The distance between the clamps was controlled.

The serpentine-structured samples were hand stretched along a ruler until it ruptured.

## CHAPTER 5

### RESULTS AND DISCUSSION

#### 5.1 Ag-PDMS Composite

The sandwich structure was fabricated in a circular glass petri-dish measuring 5 cm in diameter and total thickness of 556 $\mu\text{m}$ . The thickness of the conducting Ag-PDMS layer was measured as 47.68 $\mu\text{m}$  under an optical microscope. The optical microscopic view of the top and cross-section has been illustrated in Fig. 8, where the two transparent bounding layers are of PDMS and the thin layer in between is the Ag-PDMS composite.

##### 5.1.1 Electrical Characterization

The sheet resistance of the Ag-PDMS layer was measured with a four-point probe, from Semiprobe, to be 19.3 m $\Omega$ /sq. The resistivity of the conducting layer was calculated to be 9.202  $\mu\Omega$ -cm with the formula  $\rho = R_s * \text{thickness of the layer}$ , where  $R_s$  is the measured sheet resistance. The conductivity was further calculated with the formula  $\sigma = \rho^{-1}$  to be  $1.08 * 10^5 \text{ S cm}^{-1}$ . This is comparable to the metallic conductivity of 20  $\mu\text{m}$  thick Cu foil at  $5.8 * 10^5 \text{ S cm}^{-1}$ . The end-to-end bulk resistance of the circular disc shaped sandwich structure was measured as 1.35  $\Omega$  with a 2-point DC probe compared to 1.605  $\Omega$  measured resistance of circular disc above-mentioned Cu foil of the same diameter. This higher value of measured resistance [38] over calculated approximate bulk resistance of 0.003054 $\Omega$  of the sandwich structure is explained by the dominance of contact resistance at the junctions of the copper tab-Ag PDMS composite paste and the tab-metal probe tip contact.

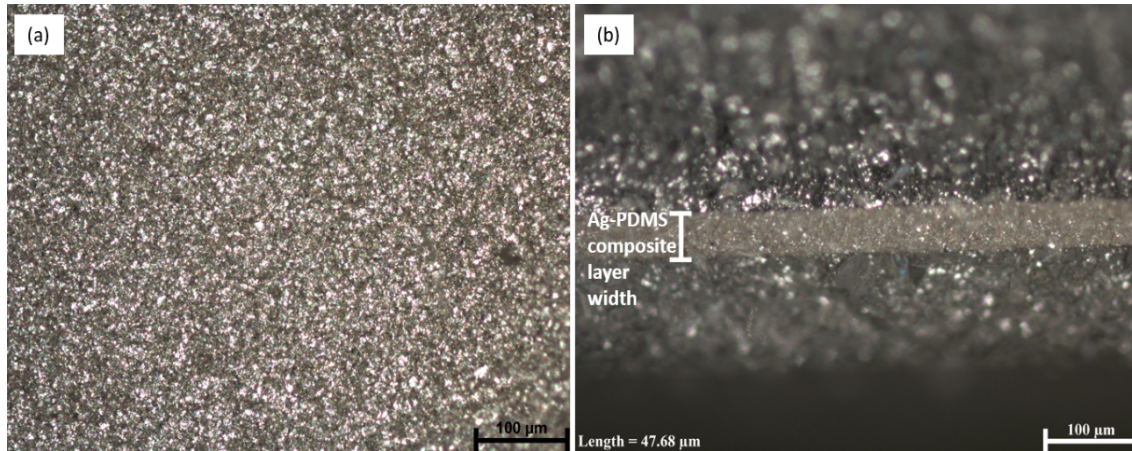


Fig. 8 (a) Optical Microscopic view of the Ag-PDMS composite layer through the transparent PDMS layer on top. (b) Cross-sectional view of the Sandwich Structure.

## 5.1.2 Mechanical Characterization

### 5.1.2.1 Bending Fatigue Test

No bent or crease was observed on the PDMS-Ag sandwich structure after 10,000 cycles at 90°. The bending radius was not considered since the sample bent over the edge of a beam as shown in Fig. 9(b). The optical microscopic images did not show any deformation of the hardened PDMS layer or the conducting Ag-PDMS paste in between. There was no significant change in resistance as well.

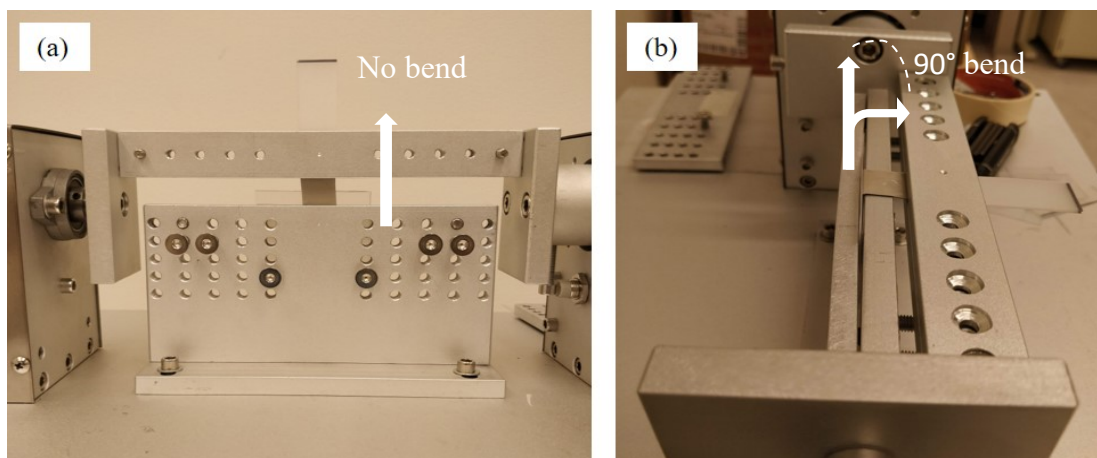


Fig. 9 (a) Sandwich structure clamped between two beams in between two polycarbonate sheets in Bending Fatigue Testing Machine when there is no bending (b) Side-view of bending over the edge of the lower beam at 90°

#### 5.1.2.2 Stretch Test

A Ta.XT texture analyzer was used to do the uniaxial stretch test. The PDMS-Ag sandwich structure stretched up to 120% its original length at  $0.01\text{mm sec}^{-1}$ , after which the structure ruptured from the point of attachment of the copper tabs into the PDMS (Fig. 11(a)). This can be explained by the PDMS polymer curing process experiencing a weak area in bonding at the contact points in an otherwise uniform structure. The optical microscopic image of the ruptured area showed no special pattern of the torn edge (Fig. 11(b)). A plot of  $\Delta R/R_0$  against strain% (Fig. 12), where  $R_0$  is the resistance at 0% strain and  $\Delta R$  is the change in resistance, showed high variance towards the beginning of stretching, but the resistance lowered with increasing strain and stabilized at around 40% elongation. After increasing the strain to 60%, the clamps of the textile analyzer had to be tightened to prevent the material from slipping, which resulted in more pressure on the Ag-Cu tab contact, thereby changing the resistance readings on the ohmmeter. The



process had to be repeated at 75% strain. This resulted in 3 different plots of the change in resistance with strain (Fig. 12). The reducing value of resistance with stretching, although counterintuitive, can be explained with percolation theory. Initially as the material stretches, the conducting particles align themselves to make a better conducting path. This conducting path stabilizes above a certain strain until hinge rupture.

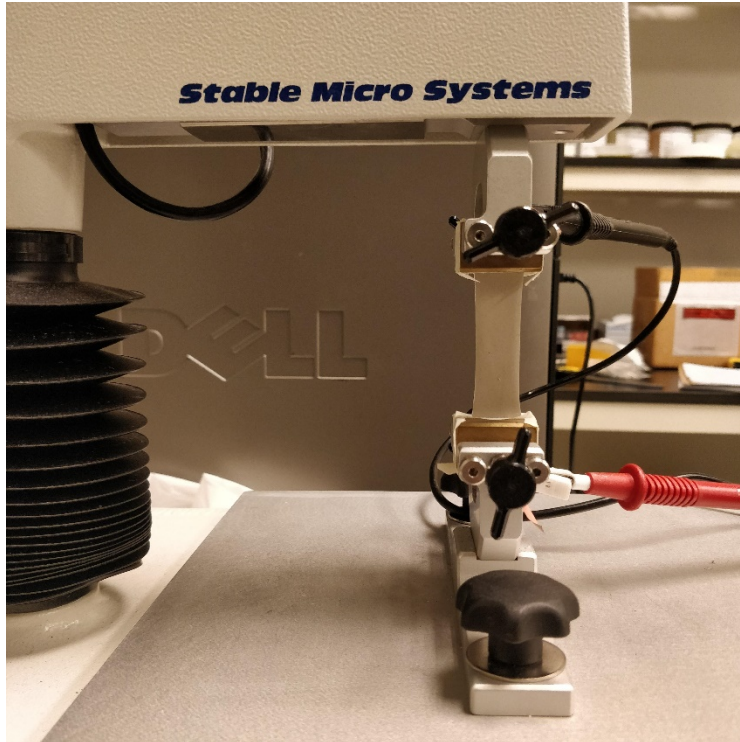


Fig. 10. Stretch test setup: The sample clamped between two ends of the textile analyser. The base is fixed, and the top clamp moves vertically to apply stress on the material. Alligator clips are attached to the cu-foil tabs coming out of the insulated clamps which connect to the probes of the two-point ohmmeter.

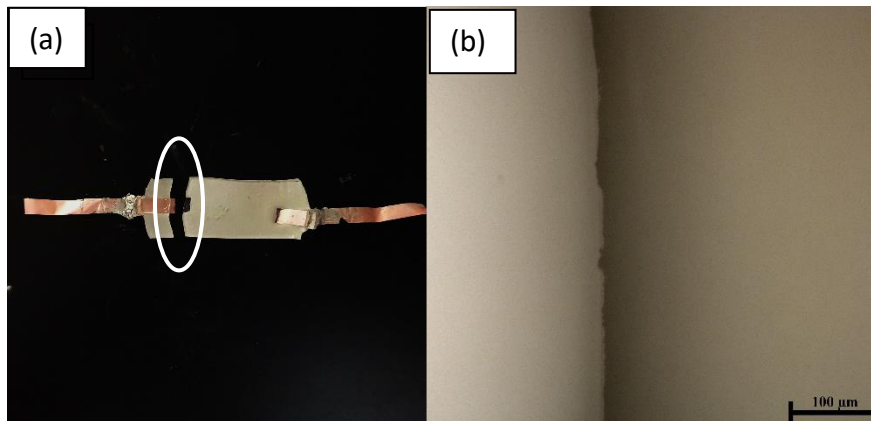


Fig. 11(a) Ruptured area of sample under test in the textile analyser (b) Broken edge under optical microscope.

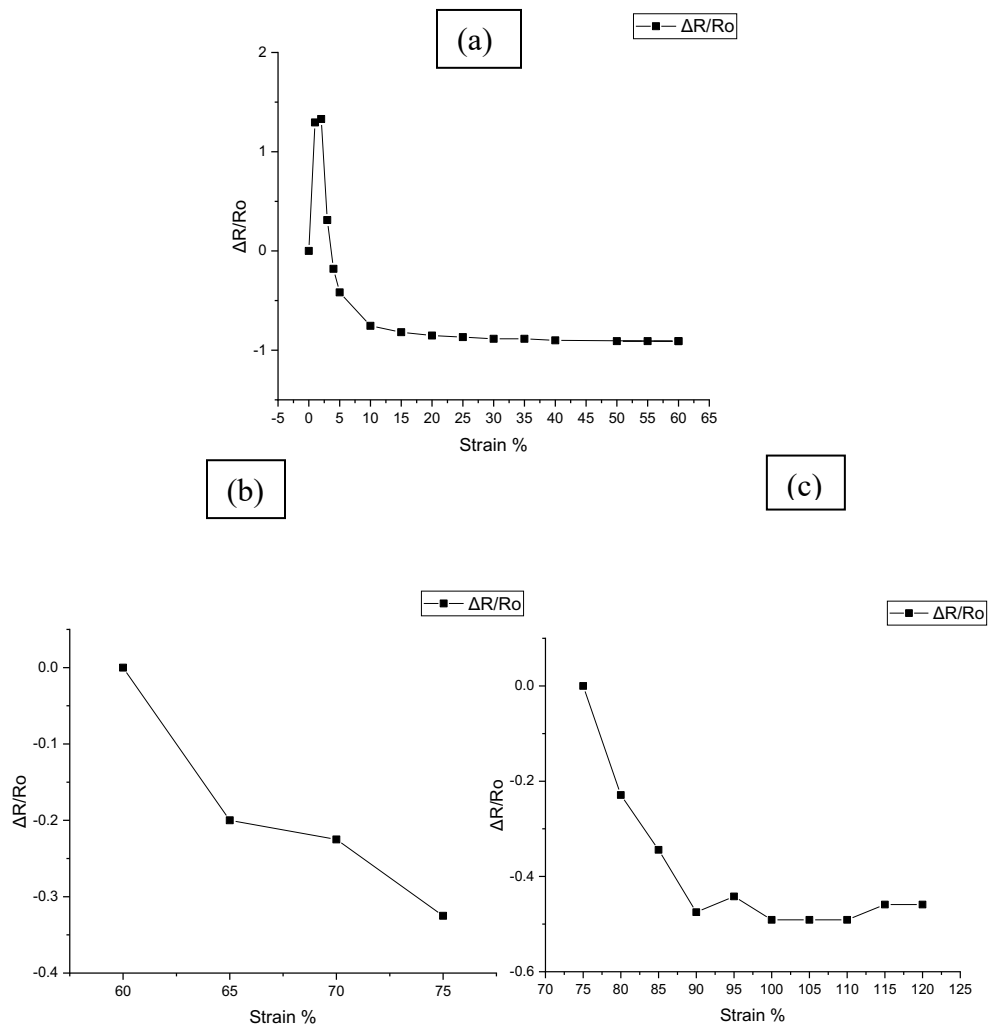


Fig. 12.  $\Delta R/R_0$  against strain% for (a) 0 to 60% strain (b) 60 to 75% strain (c) 75 to 120% strain

## 5.2 Cu Foil, Single-sided Cu Coated PI, Al Coated PET

### 5.2.1 Electrical Characterization

The measured sheet resistance of the Ag-PDMS composite using a four-point probe is compared to the sheet resistances of market-available materials in Table 2.

Material	Layer Thickness ( $\mu\text{m}$ )	Sheet R ( $\text{m}\Omega/\text{sq.}$ )	Resistivity ( $\mu\Omega \text{ cm}$ )	Conductivity ( $\text{S cm}^{-1}$ )
Ag-PDMS	47.68	19.3	9.20224	$0.108 \times 10^6$
Al coated PET	0.5	53	2.65	$0.377 \times 10^6$
Cu coated PI	18	0.958	1.724	$0.58 \times 10^6$
Cu Foil	20	0.862	1.724	$0.58 \times 10^6$

Table 2. Materials with their corresponding values of Layer thickness, Sheet Resistance, Resistivity and Conductivity. Abbreviations: PET- Polyethylene terephthalate, PI-Polyimide.

The resistivity ( $\rho$ ) is calculated with the formula  $\rho = R_s \times \text{thickness of conducting layer}$  and conductivity ( $\sigma$ ) =  $\rho^{-1}$ .

### 5.2.2 Mechanical Characterization

#### 5.2.2.1 Bending Fatigue Test

Bending Fatigue Testing Machine was used to bend the samples at  $45^\circ$  angle (Fig. 14(b)).

The material between the neutral line (along the line of maximum stress) and inner radius is under compression and the material between the neutral line and outer radius is under tension during each bent cycle. The distance between the two clamps is 1.5 cm. When bent over 10,000 cycles at  $45^\circ$  angle, Al coated PET sample developed major cracks and delamination along the line of maximum stress (Fig. 13(c), (d)). The polycarbonate sheet covers cracked, and it further pushed against the sample over multiple cycles. This can be

interpreted as a simulation of real-life conditions where batteries or devices may push against flexible interconnects over prolonged usage due to excessive bending.

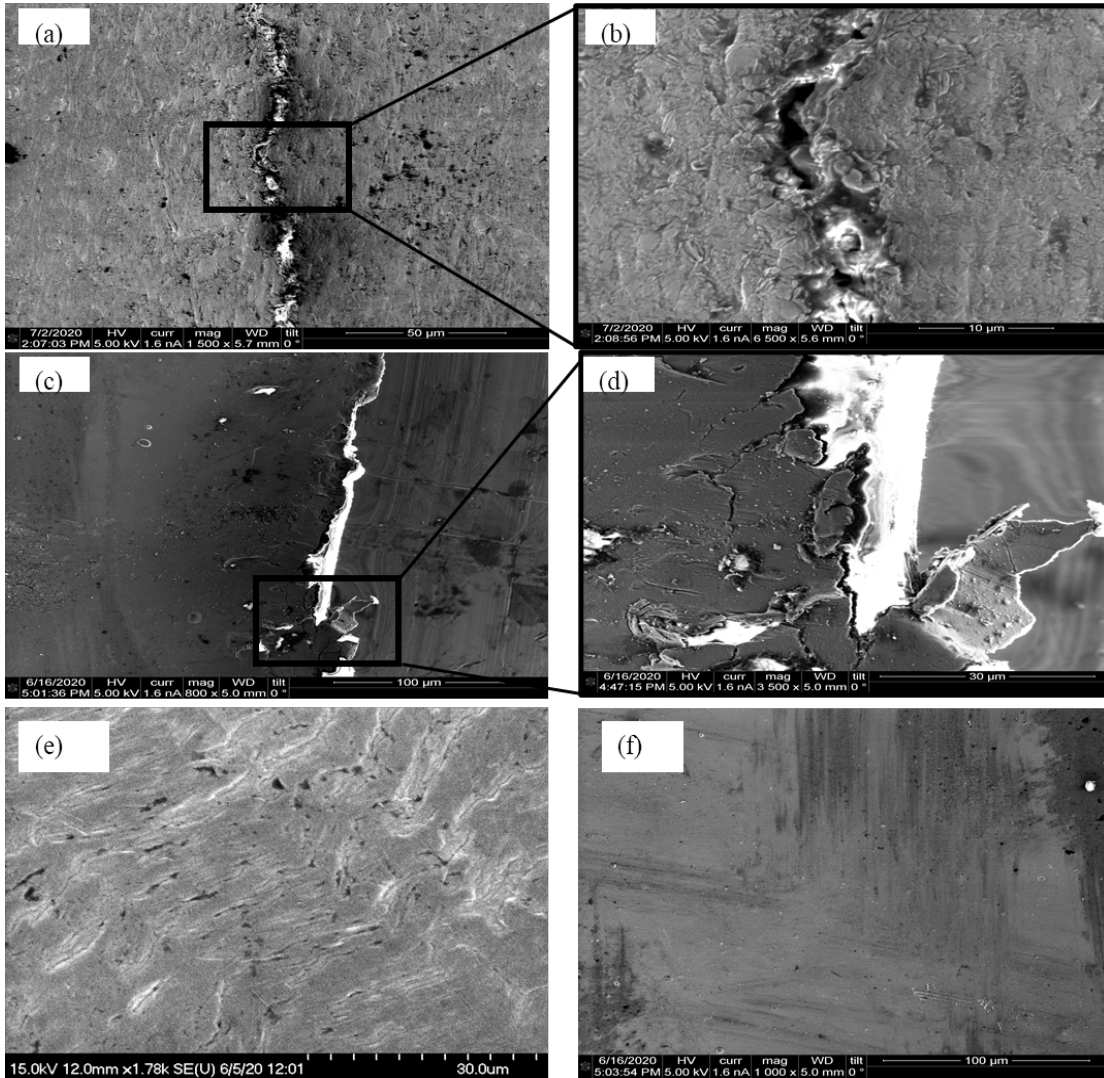


Fig. 13. SEM image of crack in (a), (b) Cu foil, (c), (d) Al coated PET (e) Cu coated PI after 10,000 bending cycles (f) Al coated PET before bending fatigue test

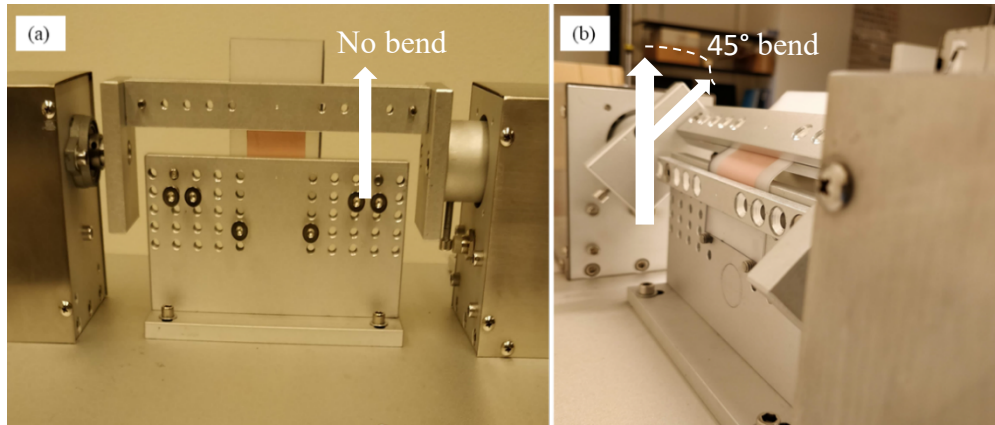


Fig. 14. (a) Front view of sample Cu foil clamped in between beams, sandwiched between polycarbonate sheets (b) Side-view of bent at 45°.

The Cu foil and Cu coated PI showed no signs of crack after bending for 10,000 cycles at 45°. The samples were then subject to sharper bending at 90° (Fig. 9(b)). While the Cu coated PI survived 10,000 cycles with no noticeable deformations (Fig. 13(e)), the Cu foil developed cracks (Fig. 13(a), (b)).

#### 5.2.2.2 Stretch Test

Neither of the three materials under test could be stretched by the textile analyzer. This matches the characteristic properties of PET and PI substrates of being almost non-stretchable by most practical means.

### 5.3 Serpentine Structure

Cu foil, Cu coated PI and Al coated PET materials are inherently non-stretchable. But they can be cut into serpentine structure which allows a longer length of the material to be folded into a smaller area of space (Fig. 15). Table 3 shows the measured resistance of unstretched serpentine structures of the samples under test and their maximum elongation percentages when hand stretched along a ruler. Measuring the end-to-end resistance of

the stretched structure was not possible due to the limitation of the sample length accommodated on the DC probe station.

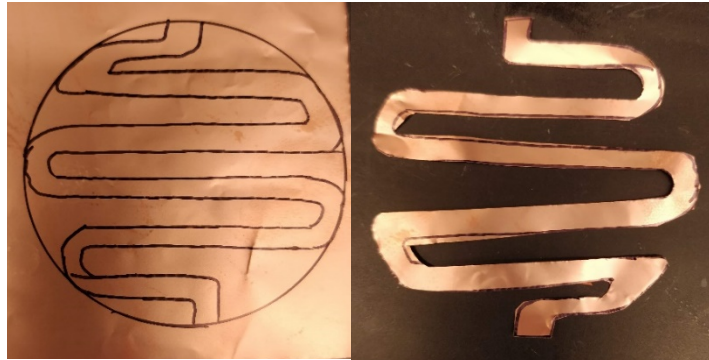


Fig. 15. Serpentine structure cut out of a Cu foil

Material	Serpentine Total Length(cm)	Measured R (Unstretched)( $\Omega$ )	Shortest length – Unstretched (cm)	Maximum Elongation %
Ag-PDMS	23.5	39.43	5	260
Al coated PET	28	5.539	5.3	277
Cu coated PI	29	13.56	5.2	303
Cu Foil	26.3	1.2	5.5	272

Table 3. Measured resistances of serpentine structures and their maximum elongation.

The high measured resistance of the Ag-PDMS sandwich structure can be explained by the non-uniform distribution of the conducting filler across the entire surface of the structure. This can further be asserted by the values of measured resistance of the circular disc shaped Ag-PDMS composite ( $1.6 \Omega$ ) being very close to metallic resistance of Cu foil ( $1.35 \Omega$ ). It can also be seen that the stretchability of the materials come at the cost of higher end to end resistance owing to the much longer actual length of the material that makes the structure.

## CHAPTER 6

### CONCLUSION

A highly conductive stretchable interconnect was prepared with 10  $\mu\text{m}$  Ag flakes and PDMS. The silver (Ag) conductive composite with polydimethylsiloxane (PDMS) as the adhesive ensured that the silver flakes were held in place in between two protective layers of mechanically robust yet stretchable PDMS. This made it electrically stable over extensive bending and stretching cycles as the conducting paths formed above the percolation threshold inside the polymer matrix remained majorly unaltered. Bulk resistance of the material was comparable within the order of magnitude of metallic conductivity of Cu foil. This structure proved to be advantageous over Cu-foil interconnects available in the market today owing to its ability to stretch and seamlessly fold without creases or cracks over multiple bending cycles. The bulk resistance also decreased with elongation. The PDMS protective layer can withstand high electronic and battery package sealing temperatures. The traditional copper foils or copper coated polyimide or aluminum coated PET sheets showed creases and could not be stretched. A closer look into the SEM images of the creases revealed a crack in the copper foil and delamination of aluminum from the PET layer. These cracks led to electrical failure. The serpentine structures cut out of circular sheets made the commercially available materials structurally stretchable, but it applied stress to the curved ends making them vulnerable to break over prolonged usage. The measured end-to-end resistance was much higher as well. Hence, the mechanically durable, electrically stable, and inherently stretchable conducting Ag-PDMS polymer composite inside a sandwich structure can be used in flexible, foldable, and stretchable electronic applications as interconnects.

## CHAPTER 7

### FUTURE SCOPE OF WORK

This work was performed under limited time frame, availability of resources and workspace due to the circumstances of COVID-19 pandemic. A few improvements to the process can be further made. The copper tab embedded in the base PDMS layer and covered with Ag-PDMS composite made an unstable contact with the conducting layer. Peeling the structure off the petri dish mechanically degraded those contacts, leading to different measurements of end-to-end resistances when taken out of the petri dish than when it was inside in ideal physical conditions. The contacts can be improved by innovating better ways to attach metal tabs within the sandwich structure. The structure can be made thinner by reducing the thickness of the protective cured PDMS layers and conducting composite. The perfect balance between the PDMS to curing agent ratio, base layer thickness and quantity of MIBK solvent in the Ag-PDMS paste can be determined by trying different combinations of the components. This aim to prepare a thinner, more stretchable interconnect can be achieved by analyzing the trade-offs between thickness, stretchability and structural feasibility. The change in conductivity and mechanical robustness should be observed over multiple stretching cycles. The composite paste can also be synthesized using silver nanowires or nanoflakes or a combination of both to ascertain if higher conductivity is achievable.



## REFERENCES

- [1] Kim, Inhyukz, et al., “*A photonic sintering derived Ag flake/nanoparticle-based highly sensitive stretchable strain sensor for human motion monitoring*”, *Nanoscale*, 10, pp. 7890, 2018.
- [2] Wen, Y. et al., “*Topological Design of Ultrastrong and Highly Conductive Graphene Films*”, *Adv. Mater.*, 29, pp. 170283, 2017.
- [3] Liu, Z. F. “*Hierarchically buckled sheath-core fibers for superelastic electronics, sensors, and muscles*”, *Science*, 349, pp. 400–404, 2015.
- [4] Lipomi DJ, Vosgueritchian M, Tee BC, et al. “*Skin-like pressure and strain sensors based on transparent elastic films of carbon nanotubes*”, *Nat Nanotechnol.*, 6(12): pp. 788-792, 2011.
- [5] “*Percolation Theory*”, Science Direct, <https://www.sciencedirect.com/topics/engineering/percolation-theory>. Accessed 20 June 2020.
- [6] Münstedt, Helmut., Starý, Zdeněk. “*Is electrical percolation in carbon-filled polymers reflected by rheological properties?*”, *Polymer*, 98, pp. 51-60, 2016.
- [7] Han, Seolhee, et al. “*High-performance, biaxially stretchable conductor based on Ag composites and hierarchical auxetic structure*”, *Mater. Chem. C*, 8, pp. 1556, 2020.
- [8] Chortos, Alex, et al. “*Mechanically Durable and Highly Stretchable Transistors Employing Carbon Nanotube Semiconductor and Electrodes*”, *Adv. Mater.*, 28, pp. 4441–4448, 2016.
- [9] Rogers, John A. et al., “*Materials and Mechanics for Stretchable Electronics*”, *Science*, vol 327(5973), pp. 1603-1607, 2010.
- [10] Maiolino, Perla. et al. “*A Flexible and Robust Large Scale Capacitive Tactile System for Robots*”, *IEEE Sensors Journal*, Vol. 13, No. 10, pp. 3910-3917, 2013.
- [11] Liao, Xinqin. et al. “*Hierarchically distributed microstructure design of haptic sensors for personalized fingertip mechanosensational manipulation*”, *Mater. Horiz.*, 5, pp. 920, 2018.
- [12] Kim, Jaemin. et al. “*Stretchable silicon nanoribbon electronics for skin prosthesis*”, *Nat. Commun.* 5:5747, 2014.
- [13] Han, Moon Jong., Dahl-Young Khang “*Glass and Plastics Platforms for Foldable Electronics and Displays*”, *Adv. Mater.*, 27, pp. 4969–4974, 2015.

- [14] Kubo, Masahiro. et al., “*Stretchable Microfluidic Radiofrequency Antennas*”, *Adv. Mater.*, 22, pp. 2749–2752, 2010.
- [15] Chen, Xiaodong et al. “*Materials chemistry in flexible electronics*”, *Chem. Soc. Rev.*, 48, pp. 1431, 2019.
- [16] Wang, Xiaolong, et al., “*Stretchable Conductors with Ultrahigh Tensile Strain and Stable Metallic Conductance Enabled by Prestrained Polyelectrolyte Nanoplatforms*”, *Adv. Mater.*, 23, pp. 3090–3094, 2011.
- [17] Xu, Feng and Zhu, Yong, “*Highly Conductive and Stretchable Silver Nanowire Conductors*”, *Adv. Mater.*, 24, pp. 5117–5122, 2012.
- [18] Zhu, Yanzhe, et al., “*Improving thermal and electrical stability of silver nanowire network electrodes through integrating graphene oxide intermediate layers*”, *Journal of Colloid and Interface Science* 566, pp. 375–382, 2020.
- [19] Sun, Yugang, et al., “*Uniform Silver Nanowires Synthesis by Reducing  $\text{AgNO}_3$  with Ethylene Glycol in the Presence of Seeds and Poly (Vinyl Pyrrolidone)*”, *Chem. Mater.*, 14, pp. 4736-4745, 2002.
- [20] Hu, Yougen, et al., “*A Printable and Flexible Conductive Polymer Composite with Sandwich Structure for Stretchable Conductor and Strain Sensor Applications*”, *ICEPT*, 18, Harbin, pp. 1361-1365, 2017.
- [21] Zhang, Bowen, et al., “*Fully embedded CuNWs/PDMS conductor with high oxidation resistance and high conductivity for stretchable electronics*”, *J Mater Sci*, 54, pp. 6381–6392, 2019.
- [22] Houghton, T., et al., “*Stretchable Capacitive Strain Sensors Based on a Novel Polymer Composite Blend*”, *ECTC*, pp. 2263-2268, 2017.
- [23] Wang, Runfei, et al., “*A highly stretchable and transparent silver nanowire/thermoplastic polyurethane film strain sensor for human motion monitoring*”, *Inorg. Chem. Front.*, 6, pp. 3119, 2019.
- [24] Zhang, Sufeng, et al., “*Highly conductive, flexible and stretchable conductors based on fractal silver nanostructures*”, *J. Mater. Chem. C*, 6, pp. 3999, 2018.
- [25] Sun, Jeong-Yun, et al., “*Highly stretchable and tough hydrogels*”, *Nature*, 489, (7414), pp. 133–136, September 6, 2012.
- [26] Zhang, Yingying, et al., “*Polymer-Embedded Carbon Nanotube Ribbons for Stretchable Conductors*”, *Adv. Mater.*, 22, pp. 3027, 2010.

- [27] Yeo, W.H., et al., “*Multi-Functional Electronics: Multifunctional Epidermal Electronics Printed Directly onto the Skin*”, *Adv. Mater.*, 25, pp. 2773, 2013.
- [28] Ge, Jin, et al., “*Stretchable Conductors Based on Silver Nanowires: Improved Performance through a Binary Network Design*”, *Chem. Int. Ed.*, 52, pp. 1654 – 1659, 2013.
- [29] Lee, Hoi-sung, et al., “*Three-Dimensionally Printed Stretchable Conductors from Surfactant-Mediated Composite Pastes*”, *ACS Appl. Mater. Interfaces*, 11, pp. 12622–12631, 2019.
- [30] Kamyshny, Alexander and Magdassi, Shlomo, “*Conductive nanomaterials for 2D and 3D printed flexible electronics*”, *Chem. Soc. Rev.*, 48, pp. 1712, 2019.
- [31] Hyun, Dong Choon, et al., “*Ordered zigzag stripes of polymer gel/metal nanoparticle composites for highly stretchable conductive electrodes*”, *Adv. Mater.*, 23, pp. 2946–2950, 2011.
- [32] Matsuhisa, Naoji, et al., “*Materials and structural designs of stretchable conductors*”, *Chem. Soc. Rev.*, 48, pp. 2946, 2019.
- [33] Choong, Chwee-Lin, et al., “*Highly Stretchable Resistive Pressure Sensors Using a Conductive Elastomeric Composite on a Micropyramid Array*”, *Adv. Mater.*, 26, pp. 3451–3458, 2014.
- [34] Ma, Rujun, et al., “*Knitted Fabrics Made from Highly Conductive Stretchable Fibers*”, *Nano Lett.*, 14, pp. 1944–1951, 2014.
- [35] Won, Phillip, et al., “*Stretchable and Transparent Kirigami Conductor of Nanowire Percolation Network for Electronic Skin Applications*”, *Nano Lett.*, 19, pp. 6087–6096, 2019.
- [36] Liang, Jiajie. et al., “*A Water-Based Silver-Nanowire Screen-Print Ink for the Fabrication of Stretchable Conductors and Wearable Thin-Film Transistors*”, *Adv. Mater.*, 28, pp. 5986–5996, 2016.
- [37] Choi, Suji. et al., “*High-performance stretchable conductive nanocomposites: materials, processes, and device applications*”, *Chem. Soc. Rev.*, 48, pp. 1566, 2019.
- [38] Mcdonald, Kirk T., “*Resistance of a disk*”, 31 March 2000, <http://www.hep.princeton.edu/~mcdonald/examples/resistivedisk.pdf>, Accessed 15 May 2020.